Mesh-free method for groundwater modeling

Jichun Li[1], C.S. Chen[1], Darrell Pepper[2], Yitung Chen[2]
[1]*Department of Mathematical Sciences,*
[2]*Department of Mechanical Engineering,*
University of Nevada, Las Vegas, USA.

Abstract

A truly meshfree method – the radial basis function collocation method is implemented for some 2-D and 3-D groundwater models. The results showed the superior simplicity, general applicability and accuracy of this method, which is a very promising simulation tool in many application areas.

1 Introduction

Since the pioneering work of Nadini and Brebbia on the dual reciprocity method (DRM) in 1982, radial basis functions (RBFs) have played an increasing important role in solving partial differential equations (PDEs) by the dual reciprocity boundary element methods (DRBEM) [1, 2], the collocation method [3, 4], and the method of fundamental solution (MFS) [5, 2].

The key features of the above RBF based methods are that they do not require a grid, which is a truly meshless method and can be used to solve complex geometry problems very easily; they can achieve high-order accuracy in a very efficient way (the implementation is very easy compared to other classic numerical methods); they are space-dimension independent due to the dimension indenpendent fact of RBFs, so they are very attractive for solving high-dimensional problems also.

Considering the simplicity, and the general applicability of the collocation method compared to DRBEM and MFS, below we only consider the RBF collocation method, which was developed by Kansa in 1990 [3]. This method has been applied to many application problems in the past decade (mainly by Kansa and Hon), such as the biphasic mixture model for tissue engineering problems, heat transfer, nonlinear Burgers' equation, shallow water equation for tide and currents simulation, and free boundary problems arising from the American option pricing. References

and details can be found in [6].

Early work of Kansa [3] and Zerroukat, Power and Chen [7] have showed that the RBF collocation method performs much better than the finite difference method (FDM). A comparison between RBF methods, and FDM, and a pseudospectral method was conducted recently by Larsson and Fornberg [8], they showed that RBF method achieved much higher-order accuracy than the pseudospectral method. Direct quantitive comparison between RBF methods and finite element methods (FEM) is being carried out recently by Li, Cheng and Chen, which show that this RBF collocation method can easily achieve superior accuracy than FEM.

The paper is organized as follows. In Section 2 we give a brief introduction to the Kansa's method. Several numerical results are presented in Section 3 for groundwater modeling in both 2-D and 3-D.

2 The RBF collocation method

This method was introduced in 1990 by Kansa [3] for solving PDEs by collocation using RBFs. This technique is very general, simple and effective. It has been successfully applied in many different areas as we mentioned in last section.

Consider a general steady-state problem in d-dimension ($d = 1, 2, 3$):

$$Lu = f(\vec{x}) \quad \text{in } \Omega, \qquad Bu = g(\vec{x}) \quad \text{on } \partial\Omega, \tag{1}$$

where L is an arbitrary differential operator, B is an operator imposed as boundary conditions, such as Dirichlet, Neumann, Robin, and mixing of them.

Let $\{P_i = (\vec{x}_i)\}_{i=1}^{N}$ be N collocation points in Ω, of which $\{(\vec{x}_i)\}_{i=1}^{N_I}$ are interior points; $\{(\vec{x}_i)\}_{i=N_I+1}^{N}$ are boundary points. The approximate solution for the problem (1) can be expressed as

$$u(\vec{x}) = \sum_{j=1}^{N} u_j \varphi_j(\vec{x}), \tag{2}$$

where $\{u_j\}_{j=1}^{N}$ are the unknown coefficients to be determined, and $\varphi_j(\vec{x}) = \varphi(||P - P_j||)$ can be any radial basis function. Here $r = ||P - P_j||$ is the Euclidean norm between points $P = (\vec{x})$ and $P_j = (\vec{x}_j)$. Most widely used radial basis functions are the multiquadric (MQ) $\varphi(r) = (r^2 + \alpha^2)^{\beta/2}$ (β is an odd integer), the Gaussians (GS) $\varphi(r) = e^{-\alpha r^2}$, the polyharmonic splines $\varphi(r) = r^n \log r$ (n is a positive even integer), and the conical type $\varphi(r) = r^n$ (n is a positive odd integer). We refer readers to the good review paper on the theory of RBF interpolation by Powell [9].

By substituting (2) into (1), we have

$$\sum_{j=1}^{N} (L\varphi_j)(\vec{x}_i) u_j = f(\vec{x}_i), \quad i = 1, 2, \cdots, N_I, \tag{3}$$

$$\sum_{j=1}^{N}(B\varphi_j)(\vec{x}_i)u_j = g(\vec{x}_i), \quad i = N_I+1, N_I+2, \cdots, N, \tag{4}$$

which can be solved for the unknown coefficients $\{u_i\}_{i=1}^N$.

For a time-dependent problem in d-dimension ($d = 1, 2, 3$)

$$\frac{\partial u}{\partial t} + Lu = f(\vec{x}, t), \quad \vec{x} \in \Omega,\ t \in (0, T) \tag{5}$$

We can construct a general θ-scheme:

$$\frac{u^{n+1} - u^n}{\delta t} + \theta L u^{n+1} + (1-\theta)Lu^n = \theta f(\vec{x}, t_n) + (1-\theta)f(\vec{x}, t_{n+1})$$

where δt is the time step, u^n $(n = 0, 1, 2, \cdots)$ is the solution at time $t_n = n\delta t$, and the parameter $\theta \in [0, 1]$.

3 Applications to groundwater modeling

Several 1-D simulations have been reported in [10], below we show some results in 2-D and 3-D.

Example 1. We consider the example of [11, p.24], which represents a cross section ($200m$ by $100m$) through a regional groundwater flow system. This model is described by the equation

$$\frac{\partial^2 h}{\partial x^2} + \frac{\partial^2 h}{\partial z^2} = 0, \quad (x, z) \in (0, 200) \times (0, 100) \tag{6}$$

with $h = 0.05x + 100$ imposed on the top boundary $z = 100m$, the side boundary conditions $\frac{\partial h}{\partial x} = 0$ at $x = 0m$ and $x = 200m$ represent regional groundwater divides, the no-flow boundary at the bottom of the system (i.e., $\frac{\partial h}{\partial z} = 0$ at $z = 0m$) represents impermeable bedrock. Here h denotes the water head.

[11] solved this model by spreadsheet modeling using 6 rows and 11 columns, the numerical solution for h is presented in a table form in [11, p.25]. We first solved this problem using the same number of nodes (i.e., 11×6 uniform grid) with r^5, the results we obtained match 3 digits of the results obtained by [11]. Since exact solution is unavailable for this model, then we solved the problem by using finer meshes 21×11 and 41×21. The obtained water head h and the flow velocity field ($u = -\frac{\partial h}{\partial x}, v = -\frac{\partial h}{\partial y}$) for these three meshes are presented in Figures 1-3, which shows that the solution converges very well with increasing collocation nodes.

Now let us consider the general transport equation

$$\frac{\partial c}{\partial t} = D_x\frac{\partial^2 c}{\partial x^2} + D_y\frac{\partial^2 c}{\partial y^2} + D_z\frac{\partial^2 c}{\partial z^2} - V_x\frac{\partial c}{\partial x} - V_y\frac{\partial c}{\partial y} - V_z\frac{\partial c}{\partial z} - \lambda c \tag{7}$$

with boundary conditions

$$c = e^{-\lambda t}(c_1 + c_2)(c_3 + c_4 e^{\frac{V_y}{D_y}y})(c_5 + c_6 e^{\frac{V_z}{D_z}z}) \quad \text{at } x = 0 \tag{8}$$

$$\frac{\partial c}{\partial x} = e^{-\lambda t}(c_3 + c_4 e^{\frac{V_y}{D_y} y})(c_5 + c_6 e^{\frac{V_z}{D_z} z}) c_2 \frac{V_x}{D_x} e^{\frac{V_x}{D_x}} \quad \text{at } x = 1 \tag{9}$$

$$\frac{\partial c}{\partial y} = e^{-\lambda t}(c_1 + c_2 e^{\frac{V_x}{D_x} x})(c_5 + c_6 e^{\frac{V_z}{D_z} z}) c_4 \frac{V_y}{D_y} \quad \text{at } y = 0 \tag{10}$$

$$\frac{\partial c}{\partial y} = e^{-\lambda t}(c_1 + c_2 e^{\frac{V_x}{D_x} x})(c_5 + c_6 e^{\frac{V_z}{D_z} z}) c_4 \frac{V_y}{D_y} e^{\frac{V_y}{D_y}} \quad \text{at } y = 1 \tag{11}$$

$$\frac{\partial c}{\partial z} = e^{-\lambda t}(c_1 + c_2 e^{\frac{V_x}{D_x} x})(c_3 + c_4 e^{\frac{V_y}{D_y} y}) c_6 \frac{V_z}{D_z} \quad \text{at } z = 0 \tag{12}$$

$$\frac{\partial c}{\partial z} = e^{-\lambda t}(c_1 + c_2 e^{\frac{V_x}{D_x} x})(c_3 + c_4 e^{\frac{V_y}{D_y} y}) c_6 \frac{V_z}{D_z} e^{\frac{V_z}{D_z}} \quad \text{at } z = 1 \tag{13}$$

and initial condition

$$c(x, y, z, 0) = (c_1 + c_2 e^{\frac{V_x}{D_x} x})(c_3 + c_4 e^{\frac{V_y}{D_y} y})(c_5 + c_6 e^{\frac{V_z}{D_z} z}) \tag{14}$$

such that we have the exact solution

$$c(x, y, z, t) = e^{-\lambda t}(c_1 + c_2 e^{\frac{V_x}{D_x} x})(c_3 + c_4 e^{\frac{V_y}{D_y} y})(c_5 + c_6 e^{\frac{V_z}{D_z} z}). \tag{15}$$

Here c is the concentration of the contaminant, $V = (V_x, V_y, V_z)$ is the seepage velocity, D_x, D_y, and D_z are the dispersion coefficients in the x, y, and z directions, respectively. λ is the rate of decay.

Example 2. Here we tested a 2-D model, i.e., $D_z = V_z = 0$ in eqn (7). For simplicity we assume that all coefficients equal one, i.e.,

$$D_x = D_y = V_x = V_y = \lambda = c_1 = c_2 = c_3 = c_4 = 1$$

In the test, we assume that domain $\Omega = [0, 1]^2$, with 32 equally distributed points on the boundary of Ω, and 9×9 uniformly distributed interior collocation points.

We tested MQ and r^5 with the same collocation points and $\delta t = 0.01$ and 800 time steps. The relative errors obtained from the fully implicit scheme ($\theta = 1$) by choosing different free parameter α in MQ are listed in Table 1, from which we see that α makes a big difference in regards of the accuracy. We found that for $\theta = 0.5$, the scheme diverges with $\alpha = 1$. We like to remark that how to choose the optimal shape parameter α in MQ is still an open problem, though much effort has been made. Hence the parameter-free radial basis functions such as $\varphi(r) = r^n \log r$ and $\varphi(r) = r^n$ are better choices in general cases. Also [12] found that MQ and GS can lead to singular coefficient matrix in some cases.

For r^5, we found that both Crank-Nicolson ($\theta = 0.5$) and fully implicit scheme ($\theta = 1$) are convergent, the accuracy are almost the same. Detailed relative errors at different time steps are listed in Table 2. The contour plots of the numerical solutions and relative errors at time steps $nt = 400$ and $nt = 500$ are presented in Figures 3-4, respectively. Note that the solutions at $nt = 400$ and $nt = 500$ differ only by a factor of e, which is observed in Figures 4-5.

Example 3. Here we tested the 3-D model of (7). and we assume that all coefficients equal one, i.e.,

$$D_x = D_y = D_z = V_x = V_y = V_z = \lambda = c_1 = c_2 = c_3 = c_4 = c_5 = c_6 = 1.$$

In the test, we assume that $\Omega = [0,1]^3$, with $11 \times 11 \times 11$ uniformly distributed collocation points. Considering the unstability of MQ we found in the 2-D problem, here we just tested r^5 with $\delta t = 0.01, nt = 800.$ The convergence history at different time steps are shown in Table 2 for both $\theta = 0.5$ and $\theta = 1.0$. The contour plots of the numerical solutions and relative errors on plane $z = 0.5$ at time steps $nt = 100$ and $nt = 200$ are presented in Figures 6-7, respectively.

Acknowledgements This work is supported by the NIA grant from UNLV Research Office.

References

[1] Partridge, P.W., Brebbia, C.A., Wrobel, L.C., *The Dual Reciprocity Boundary Element Method*, Computational Mechanics Publications: Southampton, 1992.

[2] Golberg, M.A., Chen, C.S., *Discrete Projection Methods for Integral Equations*, Computational Mechanics Publications: Southampton, 1997.

[3] Kansa, E.J., Multiquatric – A scattered data approximation scheme with applications to computational fluid dynamics II, *Computers Math. Appl.*, **19**, pp. 147–161, 1990.

[4] Franke, C., Schaback, R., Solving partial differential equations by collocation using radial basis functions, *Appl. Math. Comput.*, **93**, pp. 73–82, 1998.

[5] Fairweather, G., Karageorghis, A., The method of fundamental solutions for elliptic boundary value problems, *Adv. Comput. Math.*, **9**, pp. 69–95, 1998.

[6] Li, J., Hon, Y.C., Chen, C.S., Numerical comparisons of two meshless methods using radial basis functions, *Engineering Analysis with Boundary Elements* (in press).

[7] Zerroukat, M., Power, H., Chen, C.S., A numerical method for heat transfer problem using collocation and radial basis functions, *Int. J. Numer. Meth. Engng.*, **42**, pp. 1263–1278, 1998.

[8] Larsson E., Fornberg, B., A numerical study of some radial basis function based solution methods for elliptic PDEs, preprint.

[9] Powell, M.J.D., The theory of radial basis function approximation in 1990. *Advances in Numerical Analysis*, Vol.II, ed. W. Light, Oxford Science Publications: Oxford, pp. 105–210, 1992.

[10] Li, J., Pepper, D., Chen, Y., Chen, C.S., Mesh-free method for groundwater contamination transport modeling (submitted).

[11] Anderson, M.P., Woessner, W.W., *Applied Groundwater Modeling*, Academic Press: San Diego, 1992.

[12] Hon, Y.C., Schaback, R., On unsymmetric collocation by radial basis functions, *Appl. Math. Comput.*, **119**, pp. 177–186, 2001.

Table 1: Convergence history for MQ with different choices of the free parameter α for Example 2

Time step	$\alpha = 0.5$	$\alpha = 1.0$	$\alpha = 1.5$
20	0.00501020313	0.00083531033	0.000899423636
40	0.00525035017	0.00134056992	0.00140989565
60	0.00529006584	0.0016057118	0.00167610454
80	0.00530388485	0.00173736864	0.00178166717
100	0.00531025997	0.00180261823	0.00185893968
120	0.00531336684	0.00183485988	0.00188436906
140	0.00531489427	0.0018507162	0.00188963821
160	0.0053156462	0.00185864673	0.00191031443
180	0.00531601644	0.0018624602	0.00192094953
200	0.00531619875	0.00186425224	0.00177670536
220	0.00531628853	0.00186535349	0.00363337934
240	0.00531633273	0.00186577487	0.00313158765
260	0.0053163545	0.0018660994	0.00472031646
280	0.00531636521	0.00186625221	0.00273728648
300	0.00531637049	0.00186624756	0.00209851667
320	0.00531637309	0.00186627154	0.00327444881
340	0.00531637437	0.00186635986	0.00380790481
360	0.005316375	0.00186640468	0.0103430147
380	0.00531637531	0.00186640771	0.179788229
400	0.00531637546	0.00186639151	0.608409303
420	0.00531637554	0.00186630125	2.10549744
440	0.00531637558	0.00186628035	10.0993724
460	0.00531637559	0.00186617064	10.8669759
480	0.0053163756	0.00186617204	22.739995
500	0.00531637561	0.00186629513	598.423561
520	0.00531637561	0.00186628385	1394.38887
540	0.00531637561	0.00186625137	16568.7337
560	0.00531637561	0.0018663346	3287.76118
580	0.00531637561	0.00186635563	2717.25272
600	0.00531637561	0.00186623966	23162.0513

Table 2: Convergence history for Examples 2 and 3 solved by using r^5

Time step	2-D, $\theta = 0.5$	2-D, $\theta = 1.0$	3-D, $\theta = 0.5$	3-D, $\theta = 1.0$
20	0.00904422142	0.00589701034	0.00323852617	0.00409385173
40	0.00803439002	0.00606788254	0.00154755899	0.0055453254
60	0.00745936611	0.00613984434	0.00282533515	0.00625127541
80	0.00717591496	0.00617471752	0.00373253336	0.00659987299
100	0.00703843187	0.00619190017	0.00417315681	0.00677246403
120	0.00697188607	0.00620038678	0.00438695111	0.00685795017
140	0.00693968468	0.00620457993	0.00449067233	0.00690029517
160	0.00692410304	0.00620665183	0.00454099128	0.00692127071
180	0.00691656342	0.00620767561	0.00456540279	0.00693166093
200	0.00691291515	0.00620818148	0.00457724568	0.00693680773
220	0.00691114984	0.00620843145	0.00458299108	0.00693935719
240	0.00691029564	0.00620855496	0.00458577838	0.00694062007
260	0.00690988231	0.00620861599	0.0045871306	0.00694124563
280	0.00690968231	0.00620864615	0.00458778661	0.0069415555
300	0.00690958554	0.00620866105	0.00458810486	0.006941709
320	0.00690953871	0.00620866841	0.00458825925	0.00694178503
340	0.00690951605	0.00620867205	0.00458833416	0.00694182269
360	0.00690950509	0.00620867385	0.00458837049	0.00694184135
380	0.00690949978	0.00620867474	0.00458838812	0.00694185059
400	0.00690949721	0.00620867518	0.00458839668	0.00694185517
420	0.00690949597	0.00620867539	0.00458840083	0.00694185744
440	0.00690949537	0.0062086755	0.00458840284	0.00694185856
460	0.00690949508	0.00620867555	0.00458840382	0.00694185912
480	0.00690949494	0.00620867558	0.00458840429	0.00694185939
500	0.00690949487	0.00620867559	0.00458840452	0.00694185953
520	0.00690949484	0.0062086756	0.00458840463	0.0069418596
540	0.00690949482	0.0062086756	0.00458840468	0.00694185963
560	0.00690949481	0.0062086756	0.00458840471	0.00694185965
580	0.00690949481	0.0062086756	0.00458840472	0.00694185965
600	0.00690949481	0.0062086756	0.00458840473	0.00694185965

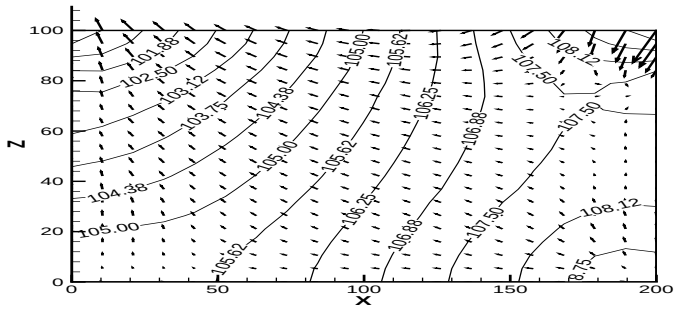

Figure 1: Contour of water head, and velocity field obtained on 11×6 grid

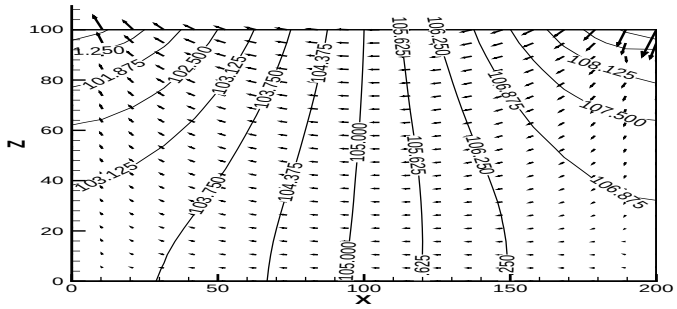

Figure 2: Contour of water head, and velocity field obtained on 21×11 grid

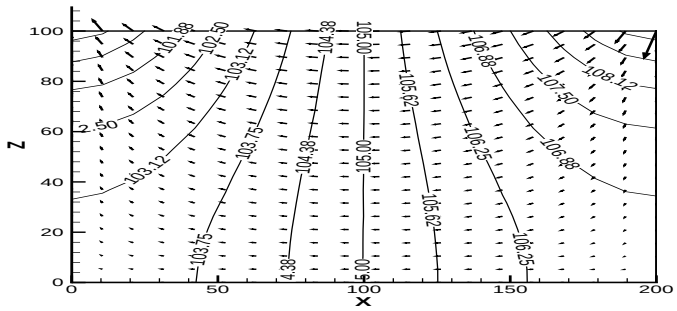

Figure 3: Contour of water head, and velocity field obtained on 41×21 grid

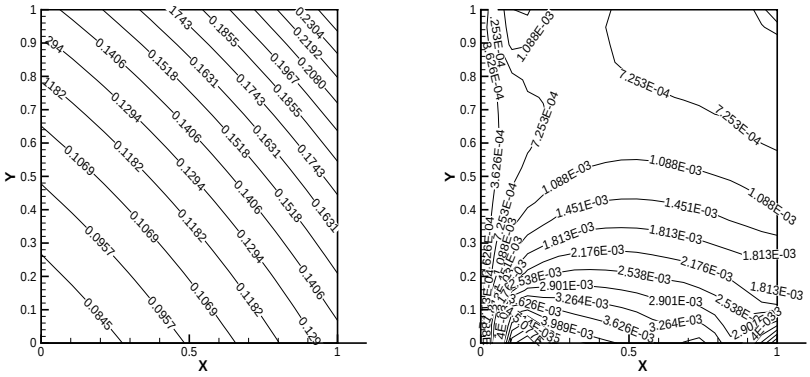

Figure 4: Contours of the numerical solution (Left) and relative error (Right) obtained for Example 2 at $nt = 400, \theta = 1$

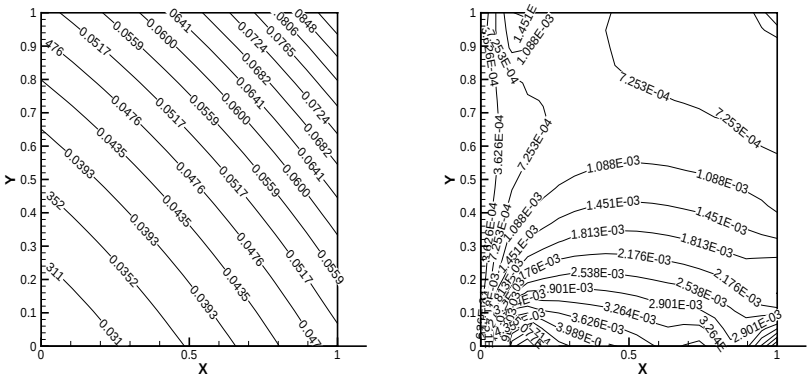

Figure 5: Contours of the numerical solution (Left) and relative error (Right) obtained for Example 2 at $nt = 500, \theta = 1$

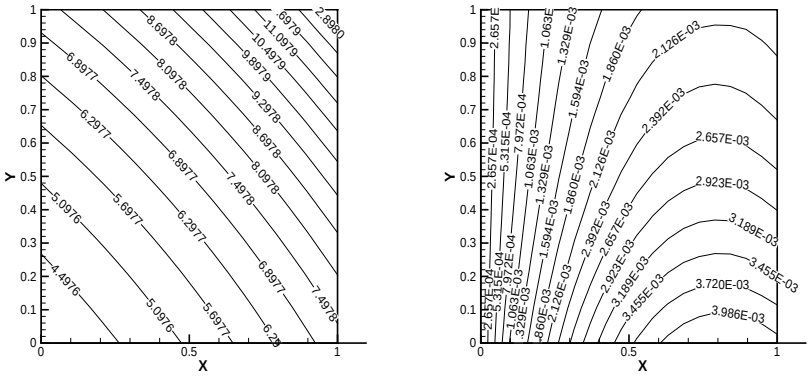

Figure 6: Contours of the numerical solution (Left) and relative error (Right) obtained for Example 3 at $nt = 100, \theta = 1$

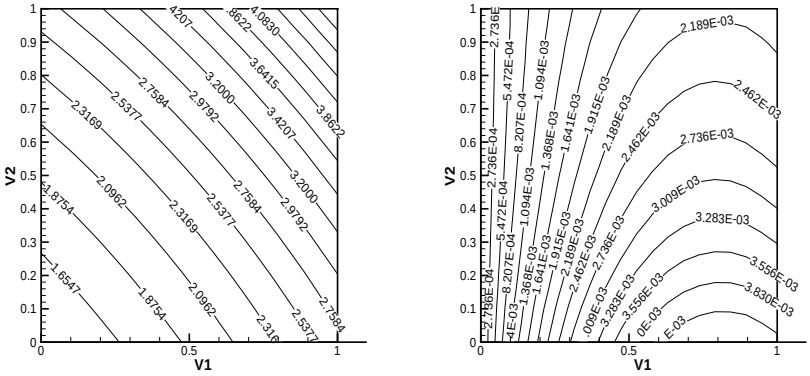

Figure 7: Contours of the numerical solution (Left) and relative error (Right) obtained for Example 3 at $nt = 200, \theta = 1$